Injection-induced thermo-poro-elasticity and boundary condition analysis for wellbore stability

Xinle Zhai & Kamelia Atefi-Monfared
Department of Civil, Structural and Environmental Engineering, University at Buffalo, Buffalo, NY, USA

ABSTRACT
Numerous studies have been conducted thus far to predict temperature and pore pressure variations within an injection layer. Available studies were developed assuming plane strain conditions, thus trivial deformations within sealing rocks. However, the response of a reservoir in the plane perpendicular to induced flow has substantial effects on in situ stress regime. Another common assumption is a content temperature at wellbore boundary from the very beginning of injection initiation. This assumption implicates a discontinuous jump in the temperature profile, from an initial state to fluid temperature. This paper presents new coupled closed-form thermoporoelastic analytical solutions for spatiotemporal pore pressure, temperature, and displacement evolutions induced in a reservoir confined with flexible sealing rocks, during early stages of injection when temperatures at wellbore change from an initial state to fluid temperature.

RÉSUMÉ
De nombreuses études ont été réalisées jusqu'à présent pour prévoir les variations de température et de pression interstitielle dans une couche d'injection. Les études disponibles ont été développées en supposant des conditions de déformation plane, donc des déformations triviales à l'intérieur des roches de scellement. Cependant, la réponse d'un réservoir dans le plan perpendiculaire au flux induit a des effets substantiels sur le régime de contrainte in situ. Une autre hypothèse courante est une température de contenu à la limite du puits de forage dès le début de l'injection. Cette hypothèse implique un saut discontinu dans le profil de température, d'un état initial à la température du fluide. Cet article présente de nouvelles solutions analytiques couplées thermoporoélastiques pour la pression porale spatio-temporelle, la température et les évolutions de déplacement induites dans un réservoir confiné avec des roches de scellement flexibles, au début de l'injection lorsque les températures passent d'un état initial à un fluide.

1 INTRODUCTION

Injection of fluids with temperatures higher or lower compared to that of the in situ strata is a typical process in numerous energy and water production and/or storage operations. The resulting alterations in in situ pore pressure and temperature have substantial effects on stress state and deformations within a rock skeleton. Heat energy transfer into a reservoir rock occurs through two different mechanisms: conductive heat transfer, and convective heat transfer (*Detournay and Cheng, 1988*; *Wang and Dusseault, 2003*). In rocks with lower permeability, fluid flow from the wellbore into the rock takes place very slowly, thus thermal energy exchange between the injectant and the solid skeleton is mainly through conduction. In rocks with high permeability, fluid flow rate into the reservoir rock is rather high. The heat energy transferred to the rock via conduction is thus insignificant, and convection becomes the main heat transfer mechanism.

Palciauskas and Domenico (1982) demonstrated the pore pressure and deformations in a rock due to the thermal loading using analytical methods. Results suggested the thermal effects to be irreversible and rather significant on pore pressure generation. *Chenevert and Salisbury (1993)* conducted a series of experiments on rock to obtain the variation of rock permeability with effective stress and porosity. Then the deformation of rock surrounding wellbore was studied in transient and steady-state flow. *Rajapakse (1993)* used Laplace and Fourier integration transforms to derive general solution for an axisymmetric stress analysis of a cylindrical borehole in an infinite poroelastic medium. The displacements, stresses and flow were presented based on modified Bessel functions of the second kind.

The simplest theory describing the coupled response of a porous strata under induced pore pressures is the theory of isothermal poroelastic consolidation, originally proposed by *Biot (1941)*. *Rice and Cleary (1976)* revised this theory considering the components' compressibility and discussed stress and pore pressure responses in plane problems. Considering only the conductive heat transfer, and assuming a constant temperature at the wellbore boundary, the solution to the general heat diffusion equation can be obtained using Laplace transform (*Carslaw and Jaeger, 1959*; *Chen and Ewy, 2005*). As the solution for temperature variations is yet complicated and difficult to implement in the field, the complementary error function has been typically adopted in the literature to obtain an approximate and simplified expression for early injection times and small radial distances from the injection source (*McTigue, 1986*; *Wang and Papamichos, 1994*).

Two fundamental sources exist behind geomechanical variations occurring during a typical injection operation: pore pressure, and heat. Pore pressures at the wellbore are believed to continuously increase with injection initiation. As for the temperatures at the wellbore boundary, the reservoir response can be assessed in two stages. (1) The stage during which the rock temperature at the wellbore boundary changes from an initial state to the fluid temperature, referred to as the first stage in this paper. (2)

The second stage during which the reservoir rock at the wellbore boundary has reached a constant temperature. Numerous studies have been dedicated on the second stage. The current paper presents new coupled closed-form thermos-poro-elastic analytical solutions for pore pressure, temperature, and deformation variations in an elastic continuum confined with flexible sealing rocks and subjected to fully-penetration injection. The proposed solutions are obtained for low permeable rocks, thus incorporating only conduction. Analogous to the study by *Monfared and Rothenburg (2017)* on flow-induced poroelasticity, the Winkler model is adopted to assess the response of the injection layer in the direction perpendicular to the injection flow. The final part of the paper presents temperature and pore pressure responses in various types of rocks in the first stage. The objective is to determine conditions in which the first stage is trivial for the analysis of wellbore stability.

2 COUPLED ANALYTICAL SOLUTION

2.1 Problem Statement

This study is aimed at deriving coupled thermoporoelastic solutions to describe the geomechanical response of an isotropic, homogeneous, semi-infinite, linear elastic continuum surrounded by flexible sealing rocks and subjected to fully-penetrating injection wellbore that generates axisymmetric radial flow (Fig. 1). The Winkler model is employed to describe the response of the injection layer perpendicular to the flow direction. Specific solution is obtained for a low permeable formation, thus incorporating only conduction as the heat transfer mechanism. Pore pressures are a function of induced temperatures, however, temperature variations are taken to be independent of pore pressures. The fluid injection flow rate is constant, and the fluid is a Newtonian fluid with a constant temperature. Assessments are carried out for drained conditions.

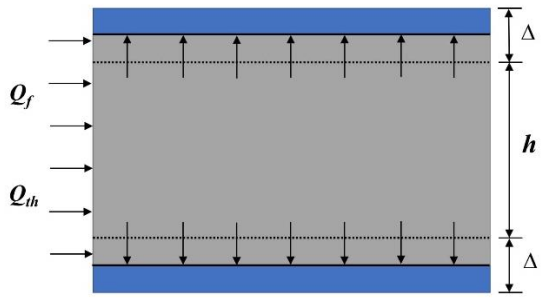

Fig. 1 Normal displacements caused by fluid injection and thermal conduction.

2.2 Analytical derivations

The thermoporoelastic constitutive equation – using the Hooke's law – adopted to describe the coupled response of an injection layer can be described as follows:

$$\sigma_{ij} = 2G_b(\varepsilon_{ij} - \alpha_t T\delta_{ij}) + (K_b - \frac{2}{3}G_D)(\varepsilon_{kk} - 3\alpha_t T)\delta_{ij} - \alpha P\delta_{ij} \quad [1]$$

where σ_{ij} is the total induced stresses; ε_{ij} is the elastic strains; δ_{ij} is the Kronecker delta; P is the induced pore pressure; T is the induced temperature ; K_b is the bulk modulus that is defined as a function of the Young's modulus (E) and Poisson's ratio (ν), $K_b = E/3(1-2\nu)$; $G_b = E/2(1+\nu)$ is the shear modulus; α is the Biot coefficient; and α_t is the coefficient of linear thermal expansion of grains.

In the vertical plane, the relation between vertical deflection (Δ) and vertical pressure (σ_{zz}) follows the Winkler model:

$$\varepsilon_{zz} = \frac{2\Delta}{h} = -\frac{\sigma_{zz}}{K} \quad [2]$$

where ε_{zz} is the elastic vertical strain on the reservoir-seal rock interface; K is the overburden Winkler stiffness parameter and defined as a function of the normal stiffness of the seal rock (K_n) and the reservoir thickness (h), namely $K = K_n h/2$ (*Monfared and Rothenburg, 2017*).

Substituting Eq. 2 into the constitutive Eq. 1, ε_{zz} can be obtained in terms of horizontal strain components, and induced pore pressure and temperatures:

$$\varepsilon_{zz} = N(\varepsilon_{rr} + \varepsilon_{\theta\theta}) - \frac{\alpha}{F}P - \frac{\alpha_t}{X}T \quad [3]$$

where ε_{rr} and $\varepsilon_{\theta\theta}$ are respectively the radial and tangential strains in the elastic state; *N*, *F* and *X* are material constants derived to be:

$$\begin{cases} N = -\dfrac{E\nu}{K(1-2\nu)(1+\nu) + E(1-\nu)} \\ F = -\dfrac{K(1-2\nu)(1+\nu) + E(1-\nu)}{(1-2\nu)(1+\nu)} \\ X = -\dfrac{K(1-2\nu)(1+\nu) + E(1-\nu)}{E(1+\nu)} \end{cases} \quad [4]$$

Combining force balance along the horizontal plane with and the constitutive equation 1, the general strain-pressure-temperature equation is derived:

$$\frac{E}{1+\nu}\left[\frac{\partial\varepsilon_{rr}}{\partial r}\left(1+\frac{\nu}{1-2\nu}(1+N)\right) + \frac{\nu}{1-2\nu}(1+N)\frac{\partial\varepsilon_{\theta\theta}}{\partial r} + \frac{\varepsilon_{rr}-\varepsilon_{\theta\theta}}{r}\right] = \left[\frac{E\nu}{F(1-2\nu)(1+\nu)}+1\right]\alpha\frac{\partial P}{\partial r} + \left[\frac{\nu}{X(1-2\nu)(1+\nu)} + \frac{1}{1-2\nu}\right]E\alpha_t\frac{\partial T}{\partial r} \quad [5]$$

Eq. 5 can be rewritten in terms of radical displacement (u_r) as:

$$\frac{\partial^2 u_r}{\partial r^2}+\frac{1}{r}\frac{\partial u_r}{\partial r}-\frac{u_r}{r^2}=\alpha Y_1\frac{\partial P}{\partial r}+\alpha_t Y_2\frac{\partial T}{\partial t} \quad [6]$$

where Y_1 and Y_2 are referred to as displacement constants and defined as follows:

$$\begin{cases} Y_1=\dfrac{E\nu+F(1-2\nu)(1+\nu)}{EF[1+\nu(N-1)]} \\ Y_2=\dfrac{\nu+X(1+\nu)}{X[1+\nu(N-1)]} \end{cases} \quad [7]$$

Integrating Eq. 6 results in a general expression for radical displacement as a function of pore pressure and temperature.

$$u_r=\frac{\alpha Y_1}{r}\int_{r_w}^{r}\Pr dr+\frac{\alpha_t Y_2}{r}\int_{r_w}^{r}Trdr+\frac{C}{r} \quad [8]$$

where C is an integral constant to be determine via boundary conditions, which can be determined by boundary conditions. Based on Eq. 3, 5 and 8, the strain components can be expressed in terms of pore pressure and temperature.

$$\begin{cases} \varepsilon_{rr}=-\dfrac{1}{r^2}\left(\alpha Y_1\int_{r_w}^{r}\Pr dr+\alpha_t Y_2\int_{r_w}^{r}Trdr+C\right)+\alpha Y_1 P+\alpha_t Y_2 T \\ \varepsilon_{\theta\theta}=\dfrac{1}{r^2}\left(\alpha Y_1\int_{r_w}^{r}\Pr dr+\alpha_t Y_2\int_{r_w}^{r}Trdr+C\right) \\ \varepsilon_{zz}=\alpha P\left(NY_1-\dfrac{1}{F}\right)+\alpha_t T\left(NY_2-\dfrac{1}{X}\right) \end{cases} \quad [9]$$

The induced stress components can then be calculated using the constitutive equation Eq. 1 and the strain components Eq. 9.

2.3 Fluid Diffusion Equation

The well-known constitutive law to describe pore pressure variations considering the thermal expansion of the saturated matrix is:

$$\frac{\partial P}{\partial t}=M\left(\frac{\partial w}{\partial t}-\alpha\frac{\partial \varepsilon_v}{\partial t}+\beta\frac{\partial T}{\partial t}\right) \quad [10]$$

where w is the variation of fluid content, M is the Biot modulus, ε_v is the volumetric strain, and β is the undrained volumetric thermal expansion. Using mass balance, the general differential equation for pore pressure is obtained as follows:

$$k\left(\frac{\partial^2 P}{\partial r^2}+\frac{1}{r}\frac{\partial P}{\partial r}\right)-\frac{1}{M}\frac{\partial P}{\partial t}=\alpha\frac{\partial \varepsilon_v}{\partial t}-\beta\frac{\partial T}{\partial t} \quad [11]$$

An expression of the volumetric strain can be obtained based Eq. 3, which would results in:

$$k\frac{\partial^2 P}{\partial r^2}+\frac{k}{r}\frac{\partial P}{\partial r}=c_1\frac{\partial P}{\partial t}+c_2\frac{\partial T}{\partial t} \quad [12]$$

where

$$\begin{cases} c_1=\dfrac{1}{M}+\alpha^2[Y_1(N+1)-\dfrac{1}{F}] \\ c_2=-\beta+\alpha\alpha_t[Y_2(N+1)-\dfrac{1}{X}] \end{cases} \quad [13]$$

The general format of equation 13 follows the traditional format, however, new expressions are obtained for coefficients of diffusivity (c_1 and c_2) which incorporate vertical confinement.

2.4 Heat Diffusion Equation

For rocks with low permeability (*Hojka, Dusseault et al. (1991)* suggest that $k<1\times10^{-18}m^2$), it is reasonable to assume trivial heat transfer and thus consider only conductive heat transfer. In this paper, heat conduction is only incorporated. Based on heat energy balance, the thermal constitutive law can be expressed as:

$$\frac{\partial T}{\partial t}=M_{th}\left(\frac{\partial \zeta}{\partial t}-\beta_{th}\frac{\partial \varepsilon_v}{\partial t}\right) \quad [14]$$

Where M_{th} and β_{th} are material constants, and $M_{th}=1/\rho C_v$. ρ and C_v are the total mass density and specific heat, and ζ is the heat stored per unit volume. In cylindrical coordinate system, Eq. 14 can be expressed in the following form:

$$K_{th}\left(\frac{\partial^2 T}{\partial r^2}+\frac{1}{r}\frac{\partial T}{\partial t}\right)=g_1\frac{\partial T}{\partial t}+g_2\frac{\partial P}{\partial t} \quad [15]$$

where

$$\begin{cases} g_1=\dfrac{1}{M_{th}}+\alpha_t\left[Y_2\left(1+N\right)-\dfrac{1}{X}\right] \\ g_2=\alpha\beta_{th}\left[Y_1\left(1+N\right)-\dfrac{1}{F}\right] \end{cases} \quad [16]$$

Assuming a particular case of $\beta_{th}=0$, which implies variations of temperature to be independent of pore pressure, results in $g_2=0$. Eq. 15 will thus simplify into the following form:

$$K_{th}\left(\frac{\partial^2 T}{\partial r^2}+\frac{1}{r}\frac{\partial T}{\partial t}\right)=g_1\frac{\partial T}{\partial t} \quad [17]$$

2.5 Solutions of Pore Pressure and Temperature

Following the approach proposed by Atefi-*Monfared and Rothenburg (2017)*, the solution for Eq. 24 can be obtained

$$T = BE_1\left(\frac{g_1 r^2}{4K_{th}t}\right) \quad [18]$$

where $E_1(I) = \int_I^\infty \frac{e^{-V}}{V} dV$ is the exponential integral, B is a coefficient related to the heat energy carried by the injected fluid.

Assuming a constant fluid injection rate (Q_{th}) and a constant fluid temperature (T_f), using the heat energy equation, and assuming small wellbore radius compared to the reservoir extension, the following relation is obtained for B:

$$B = \frac{Q_{th}}{4\pi h K_{th}} = \frac{Q_f}{4\pi h K_{th}}\left(\rho_f C_f T_f\right) \quad [19]$$

and the expression of temperature Eq. 18 turns into the following equation:

$$T = \frac{\rho_f C_f T_f}{4\pi h K_{th}} Q_f E_1\left(\frac{g_1 r^2}{4K_{th}t}\right) \quad [20]$$

Pore pressure is therefore derived to be:

$$P = AE_1\left(\frac{c_1 r^2}{4kt}\right) + m\frac{Q_f \rho_f C_f T_f}{4\pi h K_{th}} E_1\left(\frac{g_1 r^2}{4K_{th}t}\right) \quad [21]$$

where

$$m = \frac{c_2/k}{g_1/K_{th} - c_1/k} \quad [22]$$

and A is obtained via boundary conditions as:

$$A = \frac{Q_f}{4\pi h}\left(\frac{1}{k} - \frac{m}{K_{th}}\rho_f C_f T_f\right) \quad [23]$$

Substituting results in the general solution for pore pressure as a function of *t, r, T*:

$$P = \frac{Q_f}{4\pi h}\left[\left(\frac{1}{k} - \frac{m}{K_{th}}\rho_f C_f T_f\right)E_1\left(\frac{c_1 r^2}{4kt}\right) + \frac{m}{K_{th}}\rho_f C_f T_f E_1\left(\frac{g_1 r^2}{4K_{th}t}\right)\right] \quad [24]$$

When the temperature of the injected fluid equals to that of the reservoir, T_f is zero and the pore pressure equation Eq. 24 becomes

$$P = \frac{Q_f}{4\pi hk} E_1\left(\frac{c_1 r^2}{4kt}\right) \quad [25]$$

which is the solution proposed by Atefi-*Monfared and Rothenburg (2017)* for flow-induced pore pressures under isothermal conditions.

3 SPECIAL CASES

3.1 Vertical Confinement

Two limiting cases are discussed in this paper to demonstrate the significance of vertical confinement effects governed by the stiffness of sealing rock. First, very soft seal rocks are considered ($K_n \to 0$). The parameters of the proposed analytical solution become:

$$N = -\frac{\nu}{1-\nu},\ F = -\frac{E(1-\nu)}{(1+\nu)(1-2\nu)},\ X = -\frac{1-\nu}{1+\nu},$$

$$Y_1 = \frac{(1+\nu)(1-2\nu)}{E},\ Y_2 = 1+\nu$$

Next, is where the stiffness of seal rock is quite large (K_n/K_D =1000). The vertical displacement approaches zero and the reservoir rock deformation can be simplified as plane strain. The parameters of seal rock will be as follows:

$$N = 0,\ F \to -\infty,\ X \to -\infty,\ Y_1 = \frac{(1-2\nu)(1+\nu)}{E(1-\nu)},$$

$$Y_2 = \frac{1+\nu}{1-\nu}$$

3.2 Heat Transfer at Wellbore

We consider two case scenarios in terms of wellbore temperature: first stage, and second stage. First stage, where the rate of heat energy is constant, temperature response is described by the proposed Eq. 20. As for the latter stage (common approach in available studies), the complementary error function Eq. 26 is employed to get the temperature response over time and space (*Wang and Papamichos, 1994*).

$$T = T_f\sqrt{\frac{r_w}{r}}erfc\left(\frac{r-r_w}{2}\sqrt{\frac{g_1}{K_{th}t}}\right) \quad [26]$$

where $erfc(I) = \frac{2}{\sqrt{\pi}}\int_I^\infty e^{-V^2} dV$ is the complementary error function.

Fig 2 illustrates the comparison between temperature response based on the above two different boundary conditions. For the first stage with a constant heat energy rate, the temperature at wellbore boundary changes gradually from the initial temperature. As for the second stage, the temperature at the wellbore boundary jumps from the initial state to fluid temperature at the beginning of fluid injection.

All parameters are presented as normalized values in this paper: normalized time $t^* = \frac{4K_{th}t}{g_1 r_w^2}$, normalized radius

$r^* = r/r_w$ and normalized temperature $T^* = T/T_f$. t^* is assigned a very small value for Eq. 26 in order to find the temperature distribution at injection initiation. Based on the temperature expression Eq. 20, the expression of temperature can be calculated at wellbore boundary

$$T|_{r=r_w} = \frac{Q_{th}}{4\pi h K_{th}} E_1\left(\frac{1}{t^*}\right) \quad [27]$$

When T_w is equal to T_f , the heat energy can calculated from Eq. 27

$$Q_{th} = \frac{4\pi h K_{th}}{E_1\left(1/t^*\right)} \quad [28]$$

By setting normalized time a small value (1×10^{-5}) for Eq. 26, we can compare the temperature distribution at the end of the first stage with that of the beginning of the second stage from Eq. 26 (Fig 3). It shows that the difference between the temperature distribution from the two cases is large when the time of first stage is relatively long. With the time of first stage decreasing, the temperature response at the end of first stage become closer to the temperature distribution of the second stage obtained based on the error function. When the period of first stage is very short, the temperature distribution at the end of first stage is very close to that at the beginning of second stage. Hence, it is reasonable to assume that the temperature at wellbore boundary equals to fluid temperature at the beginning of injection.

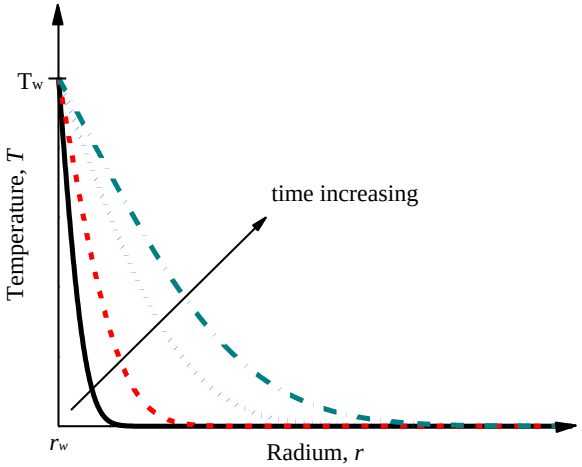

(a) constant T_w

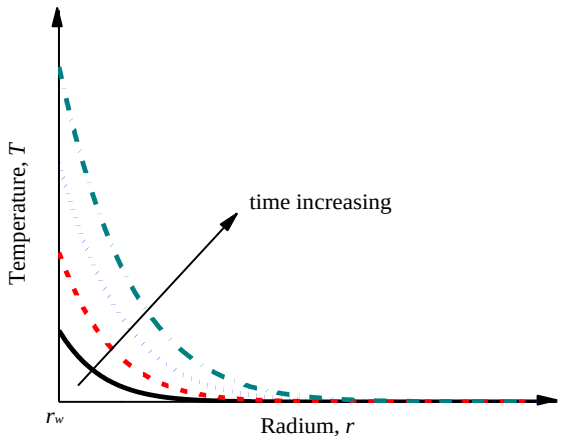

(b) constant Q_{th}

Figure 2. A schematic illustration of temperature response based on two boundary conditions.

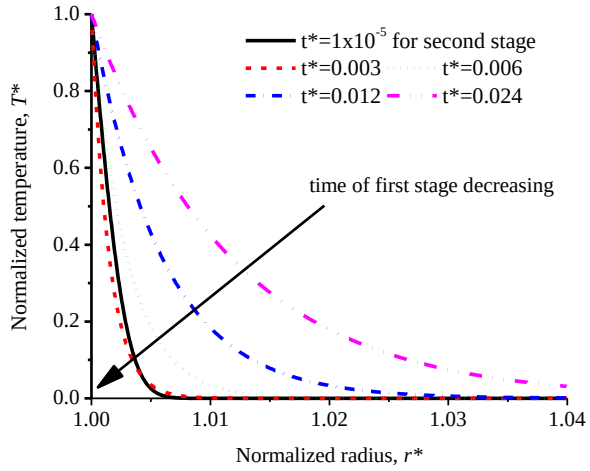

Figure 3. Temperature distribution at the end of first stage.

4 SENSITIVITY ANALYSES

4.1 Thermal effects on Pore Pressure in First Stage

Thermal effects on pore pressure alterations during the first stage are assessed next. Tab 1 presents the adopted parameters. Figs 4 and 5 present pore pressure distributions and histories. Higher pore pressures are observed when thermal effect is considered. Assuming $T_w = T_f$ in the beginning of injection, pore pressure response obtained will be significantly different.

Table 1. Parameters' values of model.

Geometry and injection data	Fluid-injected parameters	Rock properties
$r_w = 0.5m$		$E = 1\times10^{10}\,Pa$
		$\nu = 0.3$
$h = 0.67m$	$\rho_f = 1000kg/m^3$	$\rho C_\rho = 2\times10^6\,J/kg\cdot K$
$Q_f = 0.002m^3/s$	$C_f = 4200J/kg\cdot K$	$\alpha_t = 2\times10^{-6}/K$
		$k = 2\times10^{-12}m^2/Pa\cdot s$
$\alpha = 0.7$	$T_f = 100°C$	$K_{th} = 5W/m\cdot K$
$K = K_b$		$M = 2\times10^{10}\,Pa$
		$\beta = 1\times10^{-3}/°C$

4.2 Effects of Vertical Confinement

In the analysis above, the stiffness of the sealing rock K, is taken to be equal to the stiffness of the reservoir rock K_b. Next, three different case scenarios are considered to obtained the effect of K on pore pressure and stress responses in an injection process: $K = 0.1K_b$, $K = K_b$ and $K = 10K_b$. The input parameters are those presented in Tab 1 and the fluid temperature is 100 degrees. Results show insignificant effect of vertical confinement on pore pressures (Fig. 6). Pore pressure increases slightly with the increasing of K. Fig 7 gives the variations of effective stresses with different stiffness of seal rock. The induced radial stress increases and tangential stress decreases under stiffer vertical confinement settings. The vertical stress decreases rapidly under softer sealing rocks. When the stiffness of seal rock is zero, the vertical stress becomes zero and the wellbore stability becomes plane stress problems.

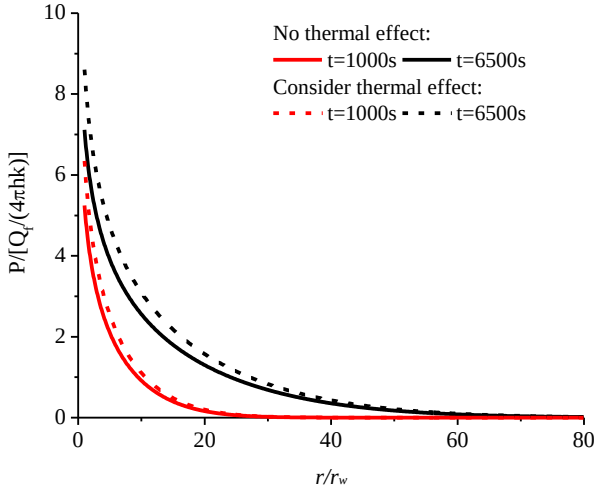

(a) Pore pressure distributions at different times.

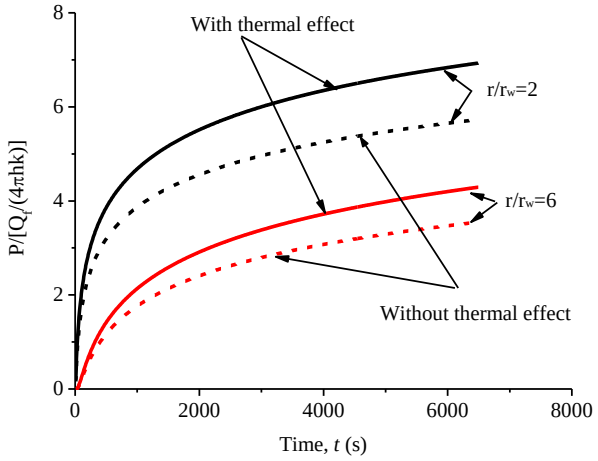

(b) Pore pressure histories at different locations.

Figure 4. Pore pressure distribution and histories, with and without thermal effects.

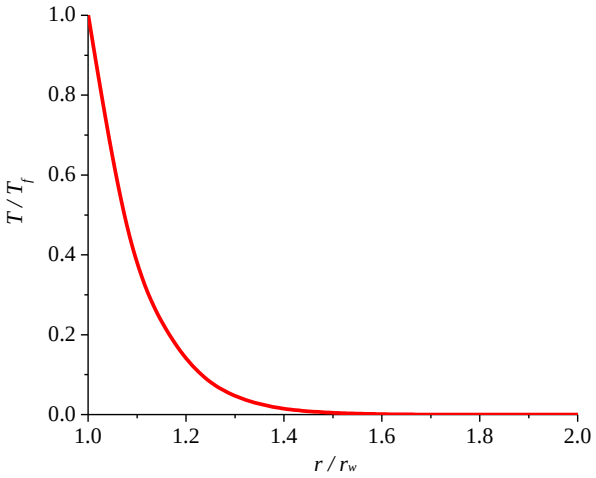

Figure 5. Temperature distribution at the end of first stage.

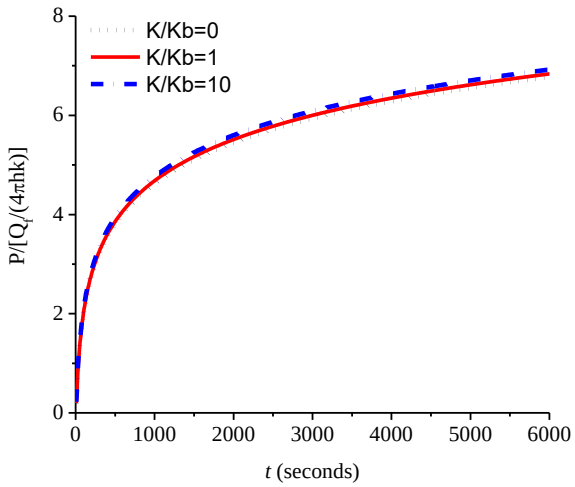

Figure 6. Normalized pore pressure history at $r/r_w=2$ for different K/K_b.

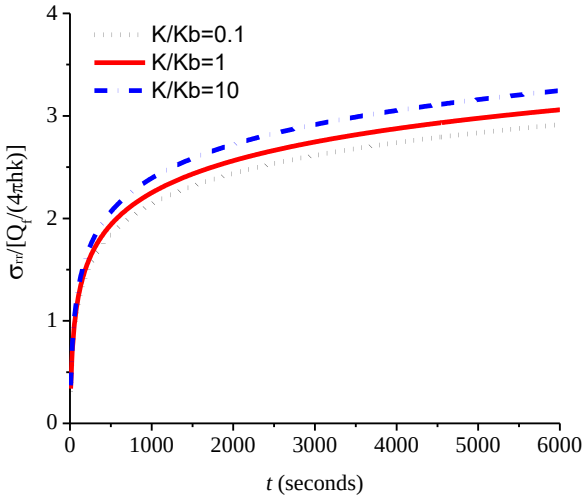

(a) Induced radial stress.

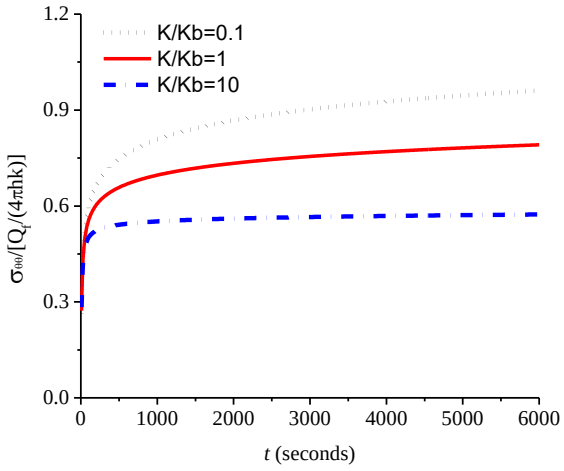

(b) Induced tangential stress.

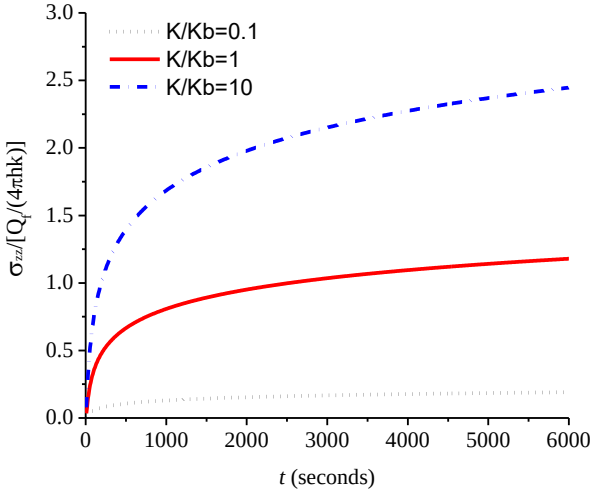

(c) Induced vertical stress

Figure 7. Induced pore pressure distribution at t=6500 seconds for different K/K_b.

5 CONCLUSIONS

This paper presents new closed-form thermo-poro-elastic analytical solutions for fluid injection in an elastic medium confined with flexible sealing rocks, assuming a constant injection rate and heat energy, incorporating only conductive heat transfer. Based on thermo-poroelastic theory and Winkler model, new fluid and heat energy diffusion equations are obtained. The analytical solutions are derived for the first stage where rock temperature at the wellbore is transient.

By comparing the temperature distribution at the end of first stage and at the beginning of the second stage, we obtain the condition that the normalized time is smaller than 0.03, under which the first stage can be neglected. The pore pressure history in the first stage is given based on the analytical solutions, which demonstrates the significance of first stage for wellbore stability. Finally, different stiffness values of seal rock are discussed and results prove that the stiffness of seal rock has a significant effect on induced effective stress response.

REFERENCE

Allen, K. G., et al. 2014. Rock bed storage for solar thermal power plants: Rock characteristics, suitability, and availability. *Solar Energy Materials and Solar Cells.* 126: 170-183.

Atefi-Monfared, K.. and L. Rothenburg. 2017. Poroelasticity During Fluid Injection in Confined Geological Reservoirs: Incorporating Effects of Seal-Rock Stiffness. *SPE Journal.* 22(01): 184-197.

Biot, M. A. 1941. General Theory of Three‐Dimensional Consolidation. *Journal of Applied Physics.* 12(2): 155-164.

Carslaw, H. S. and J. C. Jaeger. 1959. Conduction of heat in solids. London, Oxford University Press.

Chen, G. and R. T. Ewy. 2005. Thermoporoelastic Effect on Wellbore Stability. *SPE Journal.* 10(2): 121-129.

Chenevert, M. E. and D. P. Salisbury. 1993. Permeability and effective pore pressure of shales. *SPE drilling & completion.* 8(01): 28-34.

Detournay, E. and A. D. Cheng. 1988. Poroelastic response of a borehole in a non-hydrostatic stress field. *International Journal of Rock Mechanics and Mining Sciences & Geomechanics Abstracts.* 25(3).

Eppelbaum, L., et al. 2014. Thermal Properties of Rocks and Density of Fluids. Applied Geothermics**:** 99-149.

Hojka, K., et al. 1991. An analytical solution for transient temperature and stress field around a borehole during fluid injection into permeable media. Proceedings Annual Technical Meeting of the Petroleum Society of CIM, Banff, Paper No. CIM/AOSTRA.

Huotari, T. and I. Kukkonen. 2004. Thermal expansion properties of rocks: Literature survey and estimation of thermal expansion coefficient for Olkiluoto mica gneiss. *Posiva Oy, Olkiluoto, Working Report.* 4: 62.

McTigue, D. F. 1986. Thermoelastic Response of Fluid-Saturated Porous Rock. *Journal of Geophysical Research.* 91(B9): 9533-9542.

Palciauskas, V. V. and P. A. Domenico. 1982. Characterization of drained and undrained response of

thermally loaded repository rocks. *Water Resources Research.* 18(2): 281-290.
Rajapakse, R. K. N. D. 1993. Stress analysis of borehole in poroelastic medium. *Journal of engineering mechanics.* 119(6): 1205-1227.
Rice, J. R. and M. P. Cleary. 1976. Some basic stress diffusion solutions for fluid - saturated elastic porous media with compressible constituents. *Reviews of Geophysics.* 14(2): 227-241.
Wang, Y. and M. B. Dusseault. 2003. A coupled conductive–convective thermo-poroelastic solution and implications for wellbore stability. *Journal of Petroleum Science and Engineering.* 38(3-4): 187-198.
Wang, Y. and E. Papamichos. 1994. Conductive heat flow and thermally induced fluid flow around a well bore in a poroelastic medium. *Water Resources Research.* 30(12): 3375-3384.